Bright localized patterns and spikes in Kerr cavities

P. Parra-Rivas,[1] D. Gomila,[3] L. Gelens[1], and E. Knobloch[4]

[1] Laboratory of Dynamics in Biological Systems, KU Leuven Department of Cellular and Molecular Medicine, University of Leuven, B-3000 Leuven, Belgium
[2] Applied Physics Research Group, APHY, Vrije Universiteit Brussel, 1050 Brussels, Belgium
[3] Instituto de Fisica Interdisciplinar y Sistemas Complejos, IFISC (CSIC-UIB), Campus Universitat de les Illes Balears, E-07122 Palma de Mallorca, Spain
[4]Department of Physics, University of California, Berkeley CA 94720, USA

The Lugiato-Lefever equation is a mean-field model that describes the nonlinear dynamics of light circulating in fiber Kerr cavities and microresonators. In the anomalous group velocity dispersion regime two different types of localized dissipative states can appear. For low values of the intracavity phase detuning localized patterns emerge and undergo a particular type of bifurcation structure known as homoclinic snaking. However, for detuning values above a critical point the previous bifurcation structure is destroyed and a new class of localized states, known as spikes, emerge. We study this transition in detail and show that spikes undergo a new type of bifurcation structure known as foliated snaking.

Introduction

In the past ten years driven nonlinear Kerr wave-guide cavities, such as fiber cavities and microresonators, have got a lot of attention as sources for frequency combs (FCs) generation. These combs consist in very sharp equidistant spectral lines that can be used to measure light frequencies with an accuracy that has not been shown previously, open a new field in metrology with applications in many areas of science and technology [1]. The interesting point here is that these spectral combs correspond to the frequency spectra of dissipative structures (DSs) circulating inside a cavity. Using this correspondence it is then possible to study the formation, stability and dynamics of the FCs by means of their underlying DSs. The DSs can be extended, such as periodic patterns, or localized both in time and/or space. The latter are commonly called localized structures (LSs), or cavity solitons in the optical context. The different types of DSs can be described by the well known Lugiato-Lefever (LL) equation [1-3]. This model was initially derived in the context of passive diffractive cavities in the late 80's [2], and a few years later to describe waveguide cavities such as fiber cavities [3] and microresoantors [4]. Here we will focus on the study of the different types of LSs appearing in Kerr type of waveguide cavities when the group velocity dispersion is anomalous. In this regime the LSs are bright, in contrast to the normal dispersion regime where they are found to be dark. In the anomalous regime we will show that two different types of bright LSs can appear and are organized differently in terms of bifurcation diagrams [5]. The dark LSs appearing in the normal dispersion regime have been studied in detail in [6] and their bifurcation structure is different.

Once normalized the LL equation reads:

$$\partial_t = -(1+i\theta)E + i\partial_\tau^2 E + i|E|^2 E + S,$$

where E is the slowly varying envelope of the electric field circulating inside the cavity, t is the *slow time* describing the evolution in the cavity after every round-trip, and τ is the *fast time* describing the temporal structure inside the cavity. The first term on the right corresponds to the linear losses, θ is the phase detuning between the driving field and the nearest resonance of the cavity, the third term describes (anomalous) chromatic dispersion, the fourth term is the Kerr nonlinearity, and S is the amplitude of the driving field or pump. In this study we use θ and S as control parameters. The CW solution of the system E_{CW} satisfies the cubic equation $I^3 - 2\theta I^2 + (1+\theta^2)I = S^2$, with $I = |E_{\mathrm{CW}}|^2$. As a function of S, E_{CW} can be monovaluate if $\theta < \sqrt{3}$ and trivaluate otherwise. In the latter case the CW undergoes two turning points corresponding to the saddle-nodes SN_b and SN_t occurring at $I_{b,t} = (2\theta \pm \sqrt{\theta^2 - 3})/3$. Linear stability analysis about E_{CW} predicts a modulational instability (MI) occurring at $I = 1$, from where a periodic pattern arises with a characteristic wavenumber $k_c = \sqrt{2-\theta}$, that only exists for $\theta < 2$.

Localized patterns and spikes

The LSs are stationary solutions of the LL model and therefore satisfy the condition $\partial_t E = 0$. Two types of LSs can be found. In the presence of a subcritical pattern, LSs are *localized patterns* (LPs), which can be seen as a portion of the pattern embedded in a homogeneous surrounding. An example of such type of state is shown in Fig. 1A for $\theta = 1.5$. One particular feature of this state consists in the presence of oscillatory tails at either side of the central peak. In a spatial dynamics context these pulses correspond to *Shilnikov or wild* homoclinic orbits [5]. For $\theta > 2$ the subcritical pattern disappears and consequently LPs can no longer form. In this regime the typical LS corresponds to the solution shown in Fig. 1B for $\theta = 2.5$. This LS is known as *spike* and, in contrast to the LPs, this type of state is characterized by the absence of oscillatory tails. It corresponds to a *tame* homoclinic orbit in the spatial dynamics context.

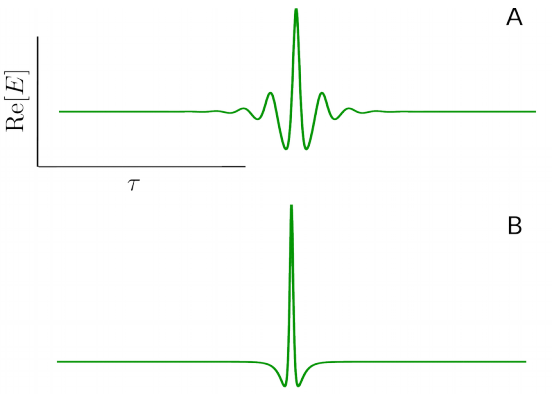

Figure 1. In A a localized pattern for $\theta = 1.5$. In B a spike type of localized state is plotted for $\theta = 2.5$.

Homoclinic versus foliated snaking

Let us now study the bifurcation structure of LPs and spikes. In order to do this we apply first weakly nonlinear multiscale analysis to obtain an approximate analytic solution of the different LSs close to a suitable bifurcation. Once this analytical solution is known we use numerical continuation algorithms to track them in any of the parameters θ and/or S to values far from the previous bifurcations. In this way we are able to calculate not only stable but also unstable highly nonlinear solutions and to build up their bifurcation diagrams. In what follow we consider a domain of size $L = 160$, and periodic boundary conditions.

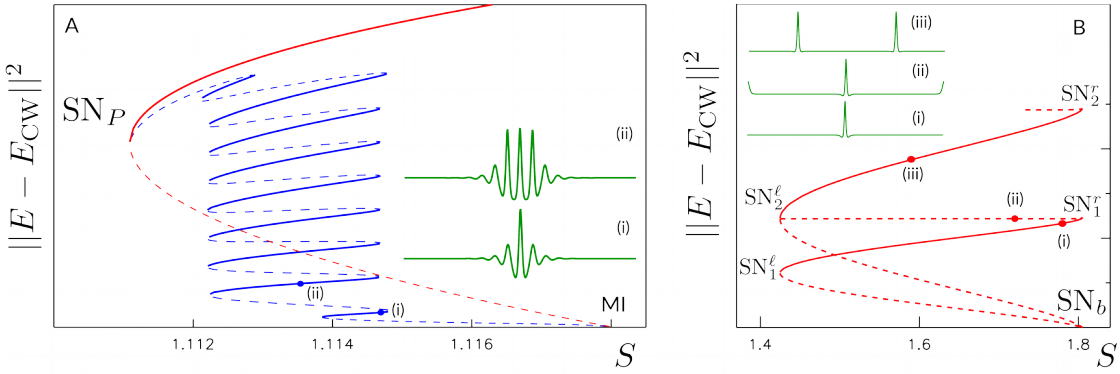

Figure 2. In panel A the homoclinic snaking bifurcation diagram is shown for the LPs for a value of detuning $\theta = 1.5$. Solid (dashed) lines correspond to stable (unstable) solutions. In B the foliated snaking type of bifurcation structure is shown for the spike solutions for a value of detuning $\theta = 2.5$.

Figure 2A shows the bifurcation diagram corresponding to the LPs. The origin of this structure is related with the presence of the MI. Weakly nonlinear analysis shows the existence of periodic pattern solutions that emerge initially stable and supercritically if $\theta < 41/30$, and subcritically and initially unstable if $\theta > 41/30$. Furthermore, the same analysis shows that in the subcritical regime two families of localized solutions of the form $E \approx E_{\rm CW} + A\mathrm{sech}(Bx)\cos(k_c x + \varphi)$ arise, where A and B depend on the control parameters of the system, and φ can take the values 0 or π. In the first case the pulses consist in a bump with the maximum at the central position (see Fig. 2A), and in the second case, they correspond to a hole with a minimum in the central position (not shown here). We can then track numerically any of the previous solutions and calculate how they modify their shape and stability when entering the nonlinear regime. The pattern, initially unstable (red dashed line), increases its amplitude as decreasing the pump S, becoming stable (solid line) in the saddle-node bifurcation $\rm SN_P$. Once this fold is passed the pattern is then stable to homogeneous perturbations for the range of parameters shown in this diagram [7]. One can also track numerically the weakly nonlinear solution corresponding to $\varphi = 0$, and as a result obtain the solution branches shown in blue. Similar to the pattern, these states are also initially stable and have small amplitude. Decreasing S the amplitude of these structures increases, and they enter a (pinning) region where the solution branches start to oscillate back and forward in S. While at the saddle-nodes on the left the structure becomes stable, at those on the right two new bumps are nucleated symmetrically at either side of the structure, which has again become unstable. While oscillating in S this process repeats continuously until, once the periodic domain is filled, the LPs connect back to the pattern. One interesting feature of this structure is that within the pinning region a wide variety of LPs coexist for the same values of the control parameters. This bifurcation structure is known as homoclinic snaking and has been found in large number of systems since it was first shown in the context of the Swift-Hohenberg equation [8].

The previous bifurcation structure is closely related to the presence of the periodic pattern arising from the MI. However, the MI disappears at $\theta = 2$. An interesting point here is to understand how the previous homoclinic snaking diagrams and its LSs modify when $\theta > 2$. Before talking about this let us first show the bifurcation structure associated to the spike LSs. Through weakly nonlinear analysis one obtains an analytical approximation of the spike solution in the neighborhood of the $\rm SN_b$ of the form $E \approx E_{\rm CW} + A\mathrm{sech}^2(Bx)$. From this formula one can already observe the

absence of oscillatory tails. The bifurcation diagram obtained once this solution is continued can be seen in Fig. 2B. The spike, initially unstable, increases its amplitude as decreasing S and becomes stable at the saddle-node bifurcation SN_1^l. The spike is then stable between SN_1^l and SN_1^r. After crossing the latter a new spike with small amplitude is nucleated at a distance $L/2$ from the previous one. Moving along this branch to the left the second spike grows in amplitude until reaching SN_2^l, where it becomes exactly the same height as the initial one. At this point this solution branch connects with two other branches, one going up corresponding to two identical high amplitude spikes separated by $L/2$ which are stable, and another going down related with two identical unstable spikes that decrease their amplitude until they disappear at SN_b. Continuing these bifurcation schemes upwards, this sequence is continuously repeated adding new spikes until filling the domain. This bifurcation structure is different from the homoclinic snaking shown previously and is called *foliated snaking* [5]. Furthermore, it shares similar features with the bifurcation diagrams of the periodic patterns as shown in [7]. In this regime LPs do also exist although their bifurcation branches are now disconnected from one another and they reconnect with the foliated snaking in a point know as Belyakov-Devaney (BD) transition [5]. One interesting feature of this BD point is that the spatial period of the pattern, and therefore the separation between peaks in the LPs diverges as approaching the BD where a global bifurcation occurs. At this point the pattern becomes a spike and the remaining branches of the homoclinic snaking reconnect with the foliated snaking. This transition has been analyzed in detail in [5].

Conclusions

In this paper we have presented a classification of the different types of LSs, and their bifurcation structures, appearing in the LL equation with anomalous group velocity dispersion. While for $41/30 < \theta < 2$, LSs correspond to LPs which undergo a homoclinic snaking bifurcation structure, for $\theta > 2$, they are spikes and organize in a foliated snaking type of structure. Moreover, LPs still exist in this regime and their solution branches follow the remnants of the homoclinic snaking which has reconnected with the foliated snaking structure.

References:

[1] P. Del'Haye, A. Schliesser, O. Arcizet, T. Wilken, R. Holzwarth, and T. J. Kippenberg, Nature (London) 450, 1214 (2007).

[2] L.A. Lugiato and R. Lefever, Spatial dissipative structures in passive optical systems, Phys. Rev. Lett. **58**, 2209–2211 (1987).

[3] M. Haelterman, S. Trillo, and S. Wabnitz, Dissipative modulation instability in a nonlinear dispersive ring cavity, Opt. Comm. **91**, 401–407 (1992).

[4] S. Coen, H.G. Randle, T. Sylvestre, and M. Erkintalo, Modeling of octave-spanning Kerr frequency combs using a generalized mean-field Lugiato-Lefever model, Opt. Lett. **38**, 37–39 (2013).

[5] P. Parra-Rivas, D. Gomila, L. Gelens, and E. Knobloch, Bifurcation structure of localized states in the Lugiato-Lefever equation with anomalous dispersion, Phys. Rev. E, **97**, 042204 (1-20) (2018).

[6] P. Parra-Rivas, E. Knobloch, D. Gomila, and L. Gelens, Dark solitons in the Lugiato-Lefever equation with normal dispersion, Phys. Rev. A **93**, 063839 (2016).

[7] P. Parra-Rivas, D. Gomila, L. Gelens, and E. Knobloch, Bifurcation structure of periodic patterns in the Lugiato-Lefever equation with anomalous dispersion, Phys. Rev. E, (accepted) (2018).

[8] P.D. Woods and A.R. Champneys, Heteroclinic tangles and homoclinic snaking in the unfolding of a degenerate reversible Hamiltonian-Hopf bifurcation, Phys. D (Amsterdam) **129**, 147–170 (1999).